The EMBO Journal Vol.16 No.14 pp.4477–4487, 1997

Intermediates in the assembly pathway of the double-stranded RNA virus ϕ6

S.J.Butcher[1,2], T.Dokland[3], P.M.Ojala[4,5] D.H.Bamford[4] and S.D.Fuller

Structural Biology Programme, European Molecular Biology Laboratory, Postfach 10.2209, 69012 Heidelberg, Germany and [4]Institute of Biotechnology and Department of Biosciences, Division of Genetics Biocenter, FIN-00014 University of Helsinki, Finland

[1]Present address: MRC Virology Unit, Institute of Virology, Church Street, Glasgow G11 5JR, UK
[3]Present address: Department of Biological Sciences, Lilly Hall of Life Sciences, Purdue University, West Lafayette, IN 47907, USA
[5]Present address: Haartman Institute, Haartmaninkatu 3, FIN-00014 University of Helsinki, Finland

[2]Corresponding author
e-mail: s.butcher@vir.gla.ac.uk

The double-stranded RNA bacteriophage ϕ6 contains a nucleocapsid enclosed by a lipid envelope. The nucleocapsid has an outer layer of protein P8 and a core consisting of the four proteins P1, P2, P4 and P7. These four proteins form the polyhedral structure which acts as the RNA packaging and polymerase complex. Simultaneous expression of these four proteins in *Escherichia coli* gives rise to procapsids that can carry out the entire RNA replication cycle. Icosahedral image reconstruction from cryo-electron micrographs was used to determine the three-dimensional structures of the virion-isolated nucleocapsid and core, and of several procapsid-related particles expressed and assembled in *E.coli*. The nucleocapsid has a $T = 13$ surface lattice, composed primarily of P8. The core is a rounded structure with turrets projecting from the 5-fold vertices, while the procapsid is smaller than the core and more dodecahedral. The differences between the core and the procapsid suggest that maturation involves extensive structural rearrangements producing expansion. These rearrangements are co-ordinated with the packaging and RNA polymerization reactions that result in virus assembly. This structural characterization of the ϕ6 assembly intermediates reveals the ordered progression of obligate stages leading to virion assembly along with striking similarities to the corresponding Reoviridae structures.

Keywords: cryo-electron microscopy/enveloped virus assembly/phi6/polymerase complex/three-dimensional image reconstruction

Introduction

Many aspects of the multi-segmented, double-stranded RNA (dsRNA) viruses, such as bacteriophage ϕ6 and the members of the Reoviridae family, raise fundamental questions about viral nucleic acid packaging and replication. In addition to RNA-dependent RNA polymerase activity, the ϕ6 polymerase complex must recognize and package one copy of each individual genomic segment to ensure that a full complement of segments is present in the virion. A further intriguing problem is the regulation of first minus strand and then plus strand RNA synthesis within this complex. The development of a unique *in vitro* reconstitution system in which the complete ϕ6 RNA replication cycle can be followed (Olkkonen *et al.*, 1990) has enhanced our understanding of these phenomena in ϕ6 replication and of similar processes in the medically important animal dsRNA viruses [reviewed in Mindich and Bamford (1988) and Bamford and Wickner (1994)]. We have now complemented these functional studies by determining the structures of the key replication intermediates of ϕ6, including the nucleocapsid (NC), the nucleocapsid core (core) and procapsid (PC), to explore the structural basis of ϕ6 replication. A summary of the compositions of these particles is shown in Table I. We have determined these structures by a combination of cryo-electron microscopy (Adrian *et al.*, 1984; Dubochet *et al.*, 1988) and three-dimensional icosahedral reconstruction (Crowther, 1971; Fuller *et al.*, 1996). The determination of these fragile structures was possible due to the preservation of their icosahedral symmetry in vitrified specimens.

Bacteriophage ϕ6 is a spherical enveloped virus of *Pseudomonas syringae* (for reviews, see Mindich and Bamford, 1988; Bamford and Wickner, 1994). The NC, consisting of the five proteins P1 (85 kDa), P2 (75 kDa), P4 (35 kDa), P7 (17 kDa) and P8 (16 kDa), is enclosed by a lipid envelope containing a further five structural proteins (Mindich and Davidoff-Abelson, 1980). Entry begins by viral attachment, followed by fusion of the viral membrane with the host cell outer membrane. Fusion releases the NC into the periplasmic space (Bamford *et al.*, 1987) from which it penetrates the cytoplasmic membrane via a membrane invagination (Romantschuk *et al.*, 1988). This second translocation requires the presence of the major NC surface protein, P8, which is removed during this process (Romantschuk *et al.*, 1988; Ojala *et al.*, 1990; Olkkonen *et al.*, 1990, 1991). This series of steps releases a transcriptionally active polymerase complex called the core into the cytoplasm (Bamford *et al.*, 1976; Kakitani *et al.*, 1980). Transcriptionally active core can be generated *in vitro* by removal of the viral envelope and the protein P8 shell (Olkkonen *et al.*, 1991).

The dsRNA genome of ϕ6 consists of three segments: small (S, 2948 bp), medium (M, 4063 bp) and large (L, 6374 bp) (Semancik *et al.*, 1973; Van Etten *et al.*, 1974; McGraw *et al.*, 1986; Gottlieb *et al.*, 1988a; Mindich *et al.*, 1988). The core comprises this segmented dsRNA genome and four protein species (P1, P2, P4 and P7) which are encoded on the L segment (Revel *et al.*, 1986; Mindich *et al.*, 1988). Distinct functions have been

Table I. Properties of ϕ6 sub-viral particles

Particle	Origin[a]	Composition	Functional properties[b]		
			Plus-strand RNA packaging	Minus-strand RNA synthesis	Plus-strand RNA synthesis
Nucleocapsid	virion	P1, P2, P4, P7, P8, dsRNA	no	no	no
Core	virion	P1, P2, P4, P7, dsRNA	no	no	yes
Procapsid	recombinant	P1, P2, P4, P7	yes	yes	yes
P1, P4	recombinant	P1, P4	no	no	no
P1	virion	P1	no	no	no

[a]See Materials and methods for purification details.
[b]Plus-strand packaging is a prerequisite for minus-strand synthesis. dsRNA is a prerequisite for plus-strand synthesis.

assigned to the four proteins. P1 has been identified as the major structural protein of this complex, forming a particle which appears dodecahedral in negatively stained specimens (Ktistakis and Lang, 1987; Olkkonen and Bamford, 1987). Plus strand RNA packaging is dependent on the presence of nucleoside triphosphates (Gottlieb *et al.*, 1991). Protein P4 has been identified as a nucleoside triphosphatase (Gottlieb *et al.*, 1992a). The presence of P7 stabilizes RNA packaging (Juuti and Bamford, 1995). After RNA packaging, the RNA-dependent RNA polymerase, P2, carries out minus strand synthesis and RNA transcription (Koonin *et al.*, 1989; Gottlieb *et al.*, 1990; Bruenn, 1991; Juuti and Bamford, 1995).

The *in vitro* system for ϕ6 RNA replication relies heavily upon the readily isolatable, functional, naive polymerase complex. The proteins of the polymerase complex can be expressed separately or in various combinations from an L segment cDNA cloned into *Escherichia coli* (Revel *et al.*, 1986; Gottlieb *et al.*, 1988b). P1 expression leads to the formation of insoluble aggregates; however, soluble dodecahedral particles can be isolated when both P1 and P4 are expressed together (Gottlieb *et al.*, 1988b). Expression of all four proteins gives rise to functional PCs that can sequentially package plus strand ϕ6 RNA, synthesize the complementary minus strand RNA and then transcribe additional plus strands which are released from the polymerase complex. Isolated cores are only capable of plus strand synthesis, despite having the same protein composition as the PCs. Both RNA-filled PCs and cores can serve as templates for P8 assembly, giving rise to infectious NCs (Gottlieb *et al.*, 1990; Olkkonen *et al.*, 1990, 1991). The availability of the different subviral particles and assembly intermediates makes ϕ6 a good system for addressing the problems of dsRNA viral assembly and determining their structural basis.

One key result of this work is the striking similarity of the bacteriophage ϕ6 structures to the corresponding ones of mammalian viruses. The NC reconstruction reveals a smooth outer shell with a $T = 13$ arrangement, similar to that of rotavirus (Prasad *et al.*, 1988; Yeager *et al.*, 1994). The core structure is reminiscent of that of reovirus cores (Metcalf *et al.*, 1991; Dryden *et al.*, 1993). These structural similarities match the shared biological properties of these segmented dsRNA viruses despite their limited sequence homology (Bruenn, 1991). The PC-related structures produced by *E.coli* expression show a number of elaborations on the dodecahedral shape described previously. Comparison of the core structure with the PC structures reveals differences in size and shape corresponding to extensive structural rearrangements and an associated expansion on maturation. We also find that PCs are metastable and undergo a partial expansion *in vitro*, in the absence of RNA.

Results

The nucleocapsid and its core

NCs were isolated from virions by removing the envelope (see Materials and methods). The NC contains proteins P1, P2, P4, P7 and an outer shell of P8 (Table I). A cryo-electron micrograph of NCs reveals smooth and rounded RNA-filled particles with an average diameter of ~58 nm (Figure 1A, black arrows). This morphology made the identification of the initial orientations problematic, although the cross-correlation method (Baker and Cheng, 1996) was effective once a model was constructed by the common lines approach.

The double-shelled nature of the NC is apparent in partially disrupted particles (Figure 1A, white arrow), where an internal, angular layer is seen. Comparison of NCs (Figure 1A) with the isolated cores (Figure 1B) shows that the outer layer corresponds mainly to the major NC surface protein P8, while the inner corresponds to the four proteins and dsRNA of the core. P8 can be released from the NC by treatment with EGTA. This results in cores (Figure 1B) which appear rounded with a number of small densities protruding from the surface (Figure 1B, small black arrows). These densities extend to a radius similar to that of the NC surface (29 nm), suggesting that a proportion of the surface of the NC is occupied by core proteins. The distribution of these densities suggests that they are located on the icosahedral 5-fold axes. The average diameter of the body of the core is ~50 nm, which matches that of the inner layer of the NC.

A 2-fold view of an NC reconstruction (Figure 2A) made from 24 particles to a resolution of 3.2 nm reveals the smooth outer layer arranged on a holey net with $T = 13$ symmetry (Caspar and Klug, 1962). This arrangement is illustrated schematically on a facet of the NC reconstruction, viewed down a 3-fold axis (Figure 2B). There are three different types of holes on the surface, denoted I, II and III, giving an appearance similar to that of the spikeless rotavirus (Prasad *et al.*, 1988). Difference imaging with the core (see below) reveals the single layer of P8 (Figures 2C, 3, 4A and B) which forms the majority of the outer NC surface. Negative staining previously demonstrated similar 10 nm holes in P8 assemblies derived by NC

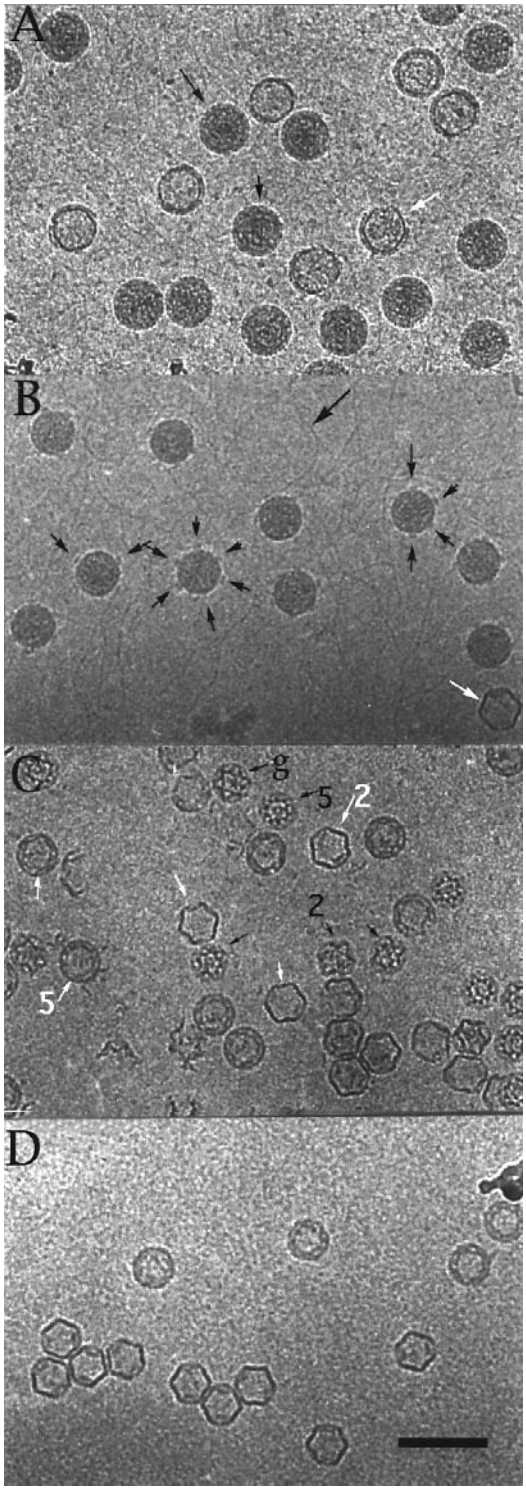

Fig. 1. Cryo-electron micrographs of the different polymerase complex-related particles. (**A**) The NCs are indicated by black arrows. The white arrow points to a partially disrupted NC where the angular inner layer, corresponding to the core, is visible. (**B**) A field of the cores, isolated from the virion. The small arrows indicate the positions of the extensions projecting out from the surface of the cores. In favourable positions, a maximum of six projections can be seen. The large arrow points out a strand of RNA in the background. The white arrow indicates a core which has lost its RNA. (**C**) A field of recombinant P1, P4 particles in unexpanded (black arrows) and expanded (white arrows) conformations. '5', '2' and 'g' indicate particles in 5-fold, 2-fold and general (non-axial) orientations respectively. (**D**) The P1 particles isolated from the virion. The scale bar represents 100 nm.

disruption or P8 self-assembly in the presence of calcium ions (Ktistakis *et al.*, 1988). Individual monomers of the 16 kDa protein P8 within the structural units of the surface cannot be resolved at the present resolution. However, the hexavalent nature of the type II and type III holes yields an estimate of the number of copies of P8. We assume, as in the case of the other $T = 13$ structures described thus far in the literature, that there are six subunits around each hexavalent hole. However, the difference map showing just P8 (Figure 2C) illustrates that approximately one-third of the density around the type II hole is occupied by core proteins. Hence, we assume that P8 occupies only four out of a possible six positions here. This gives a total of 600 P8 units in the lattice, each of which could be an oligomer of P8. The volume which would be occupied by 600 copies of the P8 polypeptide (assuming a protein density of 1.3 g/cm^3) is too small to account for the density shown in Figure 2C. The volume shown in Figure 2C corresponds to a total of 19.2 MDa or 1200 copies of P8. Hence the observed 600 P8 units probably correspond to dimers. Analytical ultracentrifugation measurements and equilibrium labelling experiments gave a value of 16.9 MDa or 1056 P8 monomers (Day and Mindich, 1980), consistent with our interpretation.

Figure 3 shows a reconstruction of the core isolated from the virion (made from 28 particles to 3.2 nm resolution). This reconstruction is nearly spherical, with a turret projecting from each 5-fold axis. These turrets correspond to the small projecting densities observed in the micrographs (Figure 1B). They are tethered to the body of the core by five slim connections, spaced ~2 nm apart. The turret is penetrated by an axial channel, as shown in the cutaway view in Figure 3B. The diameter of the channel is ~2 nm at its narrowest point. The highest T number that can be assigned to the core at this resolution is $T = 1$.

Comparing the NC and core reconstructions reveals that the ring of density around the 5-fold axis on the surface of the NC reconstruction is contributed by the turret of the core (Figures 2A, 3A, 4A and B). The remainder of the core mass (orange in Figure 4A and B) lies underneath the P8 layer (white in Figure 4A and B), and is visible through the holes in this layer. A section through the NC reconstruction shows the double-layered nature of the NC (Figure 4C, left-hand side). The core only has a single layer (Figure 4C, right-hand side). Figure 4 also shows the contact points between the P8 layer and the core. There are contacts between the two layers near the icosahedral and local 2-fold axes, indicated by white arrows in Figure 4C. Obviously there is also a major interaction around the 5-fold axes of symmetry between the turret of the core and the P8 layer where the core forms part of the NC surface (Figure 4A, arrow).

The ϕ6 procapsid

PCs were made by expressing an L segment cDNA (Gottlieb *et al.*, 1988b) in *E.coli* as described in Materials and methods. The particle produced was not stable, having a tendency to lose some of its components. The minimum requirement for particle assembly is the presence of both P1 and P4 (Gottlieb *et al.*, 1988b), which produces the PC-related P1, P4 particle. Our description of the PC structure is based primarily on the P1, P4 particle, although

the overall features are common to all the PC-related particles (P1, P2, P4; P1, P4, P7; P1, P2, P4, P7; data not shown) that we have studied.

Figure 1C shows a cryo-electron micrograph of a P1, P4 preparation. The particles have a diameter of ~46 nm and display three characteristic views (Figure 1C, black arrows): a ring of 10 dense spots surrounded by a fainter ring, a hexagonal outline and a 'star of David'. These views reflect the PC's dodecahedral shape (Mindich and Davidoff-Abelson, 1980; Steely and Lang, 1984; Yang and Lang, 1984) and correspond to a 5-fold view, a 2-fold view and a general (non-axial) view respectively. A dodecahedron shares icosahedral (532) symmetry with an icosahedron; the symmetry axes are the same. However, the dodecahedral object has 12 pentagonal faces instead of the 20 triangular ones of an icosahedron.

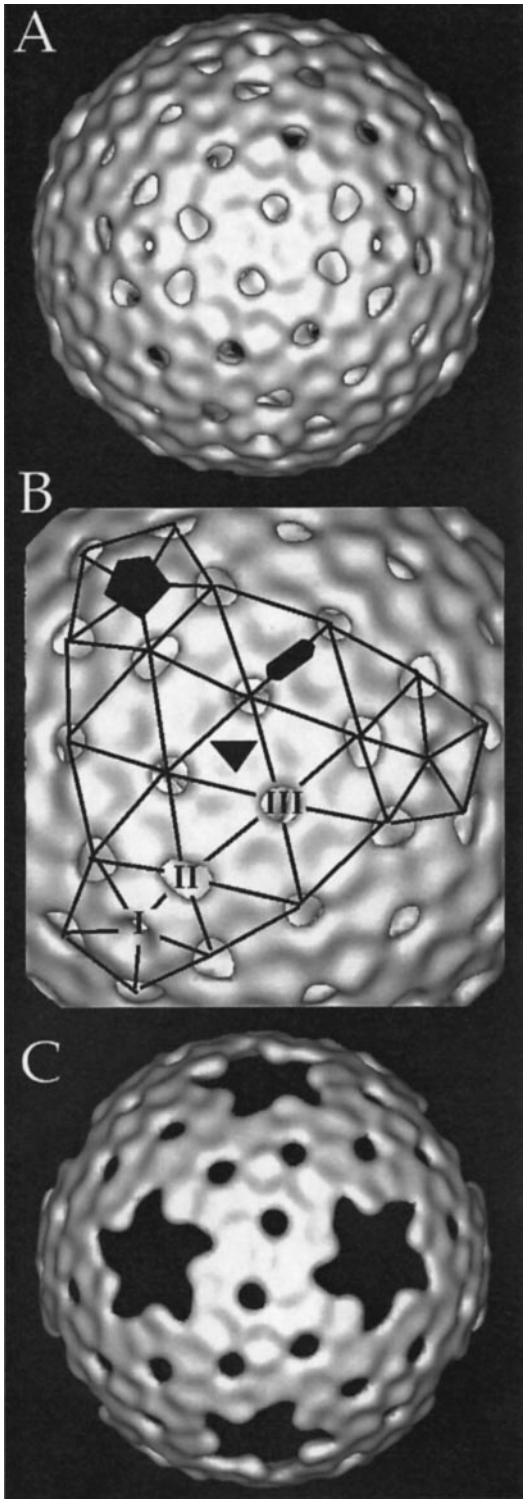

The particles exhibited a marked preference for the 5-fold view, while 3-fold views were virtually absent. This is perhaps not surprising in view of the flat surface that the pentagonal face of a dodecahedron presents to the environment. Unfortunately, the multitude of 5-fold views does not contribute much independent information to the reconstruction (Crowther, 1971). This problem was overcome by tilting the specimen by 10–15° before taking the low dose image so that a broader range of projections was obtained (Stewart *et al.*, 1991).

A reconstruction of the P1, P4 particle viewed down a 2-fold axis is shown in Figure 5A and B. This reconstruction was made from 14 particles to a resolution of 3.5 nm. The dodecahedral framework is immediately apparent, defining the overall shape of the particle. This framework consists of 30 twisted bars connected at the 3-fold axes (Figure 5A and B). The most striking elaboration on this basic scheme is the presence of 'cups' on each of the 5-fold axes, suspended from the bars of the dodecahedral skeleton. In the inside view (Figure 5B) the cups are seen to terminate in a projecting domain. The cups are responsible for generating the ring of 10 dense spots seen in the 5-fold views (Figure 1C).

The PC structure is labile. Elevating the sample tempera-

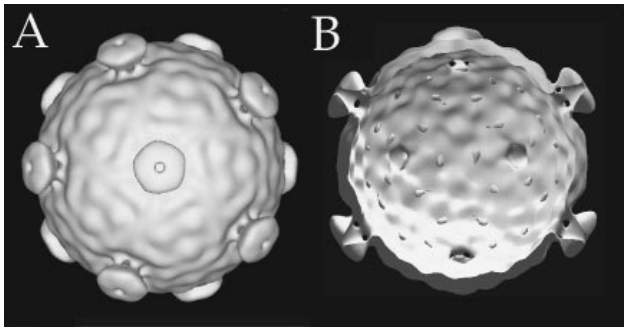

Fig. 3. Surface representation of the reconstructions of the core (**A**) viewed down an icosahedral 5-fold axis of symmetry; (**B**) a cut-open representation showing the inner surface of the structure viewed down a 2-fold axis of symmetry.

Fig. 2. Surface organization of the NC. (**A**) A surface representation of the NC reconstruction viewed down an icosahedral 2-fold axis of symmetry. The particle has two distinct layers; the inner layer can be glimpsed through the 132 holes present in the outer layer. Only the front hemisphere of the structure is shown. (**B**) A close-up of the NC surface viewed down an icosahedral 3-fold axis of symmetry (black triangle). A 2-fold (black oval) and a 5-fold (black pentagon) axis are also marked. A partial $T = 13$ lattice and the three different types of holes penetrating the surface (I, II and III) are marked. There are 120 hexacoordinated holes: 60 5-fold-adjacent holes (type II) and 60 3-fold-adjacent holes (type III). (**C**) Surface representation of a difference map calculated by subtraction of the core reconstruction from the NC reconstruction viewed down an icosahedral 2-fold axis of symmetry. Only the front hemisphere is shown. This volume reveals the position of the major NC surface protein P8 (16 kDa). The NC surface comprises rings of P8, except the ring on the 5-fold axis which is composed of core proteins. The cut-off level is ~1.5 standard deviations above the mean density level, which gives a volume corresponding to ~1200 copies of P8.

ture from 4 to 22°C caused a gradual change in particle appearance. The heat-treated particles are ~8% larger in diameter and display fewer internal features (Figure 1C, white arrows). Two distinct views of this larger particle dominate: 5-fold views which display two concentric rings and 2-fold views which show a simpler, more hexagonal outline than the original PC (Figure 1C). Thus, gentle heat treatment of PCs causes their expansion and other structural changes.

A reconstruction of these expanded particles was made from 12 particles to 3.8 nm resolution and is shown in Figure 5C and D. The expanded particles display the outline of a dodecahedral cage similar to that of the PC (Figure 5A and B), but the bars of the cage have moved outward and widened, giving the particle an inflated appearance (Figure 5C and D). The cups now appear as shallow depressions on the 5-fold axes, and show no protruding domain (Figure 5D).

Particles containing P1 alone cannot be isolated from the recombinant system due to instability and non-specific

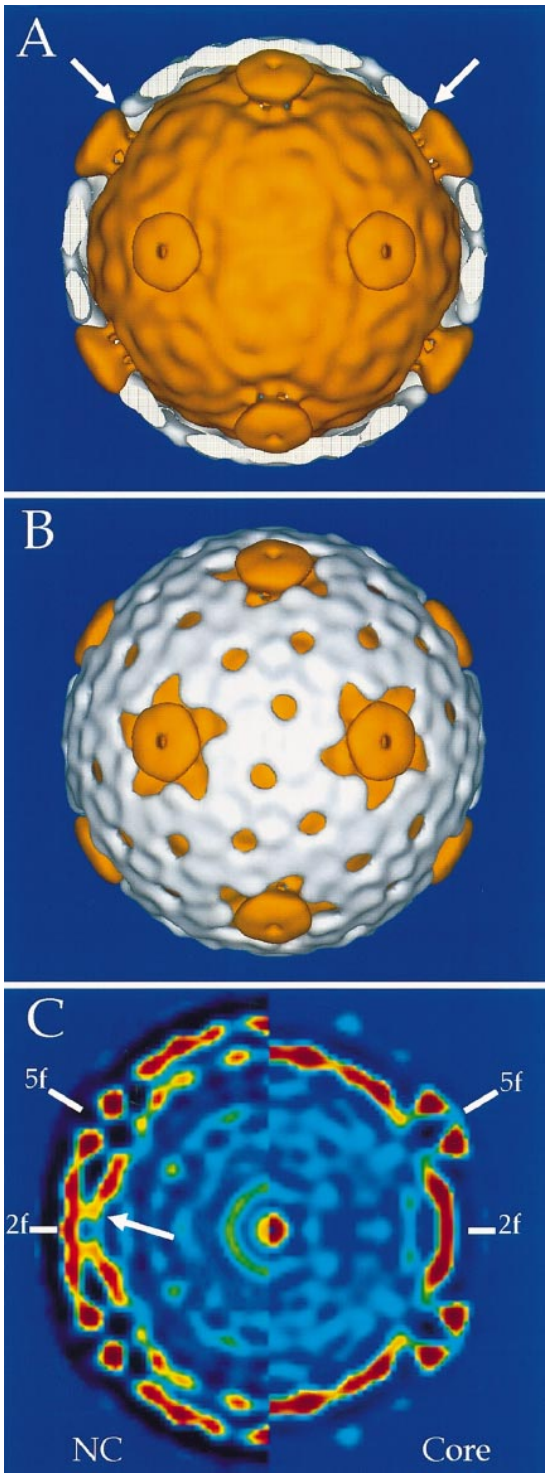

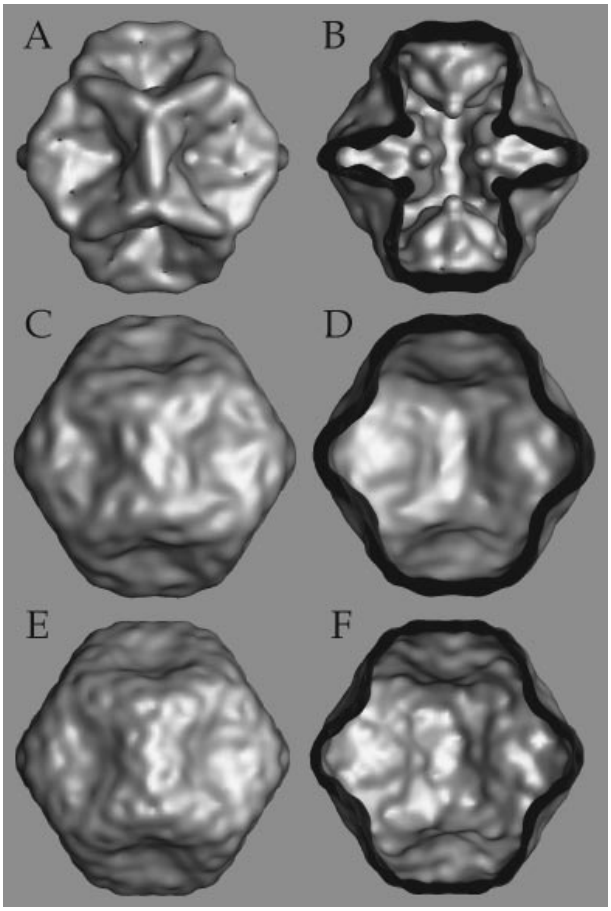

Fig. 5. Surface representations of the reconstructions of the polymerase complex-related particles. (**A** and **B**) The unexpanded P14 particle; (**C** and **D**) the expanded P14 particle; (**E** and **F**) the P1 particle. All reconstructions are shown in the 2-fold view. (A, C and E) External views; (B, D and F) cut-away views showing the inner surface.

Fig. 4. Comparison of the NC and the core reconstructions. (**A**) A surface representation of the core (in orange) inserted into a cut-away surface representation of the P8 volume (in white) showing the internal connection of the P8 shell to the core around the 5-fold tower of the core. (**B**) A surface representation of the core (in orange) inserted into a surface representation of the P8 volume (in white) showing the contribution of the core to the NC. This also highlights the surface exposure of the core within the NC. (**C**) Central sections through the NC (left-hand side) and the core reconstructions (right-hand side). P8, which forms the majority of the outer layer of the nucleocapsid, is released by chelation of calcium ions. These sections illustrate the resulting major conformational changes; the 5-fold tower is freed from contact with P8, and the connections from the core to P8 on either side of the 2-fold axis are lost, leaving no obvious protuberances at this position. There is some concentric density just above the background level inside both reconstructions which may correspond to loosely ordered RNA and/or protein. High density is red, low density is black.

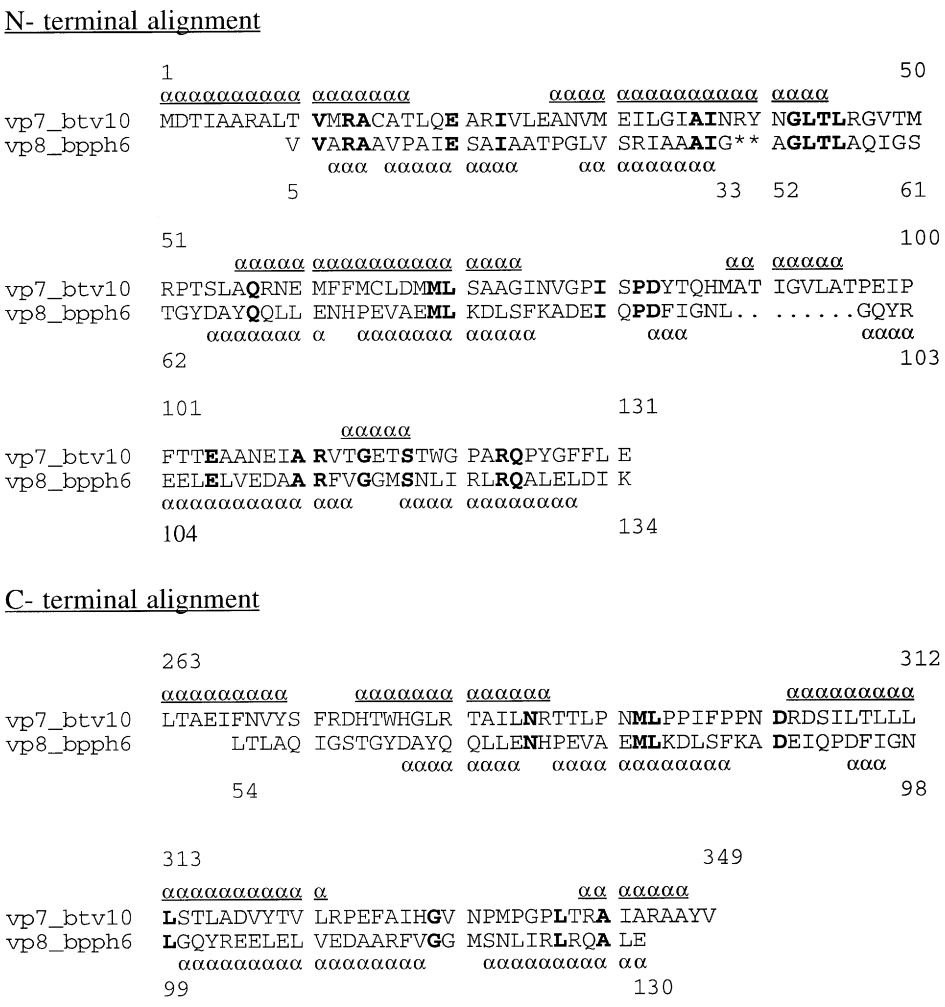

Fig. 6. Amino acid sequence comparison between blue tongue virus VP7 (SwissProt accession no. vp7_btv10) and ϕ6 P8 (SwissProt accession no. vp8_bpph6). The N-terminal alignment is between residues 1–131 of VP7 and residues 5–134 of P8. The C-terminal alignment is between residues 263–349 of VP7 and 54–130 of P8. ** marks a deletion in the P8 sequence of 19 residues to improve the N-terminal alignment. In addition, a gap was inserted in the P8 sequence between residues 99 and 100 of P8, indicated by full stops. Residues in known α-helices of VP7 (Grimes *et al.*, 1995) are marked by αs. Residues which are predicted to have an α-helical secondary structure in P8 (probability ⩾0.8) are indicated by α (Rost and Sander, 1993, 1994; Rost, 1996). Homologous residues are highlighted in bold.

aggregation *in vivo* (Gottlieb *et al.*, 1988b). However, they can be isolated from the virion in the presence of high salt (see Materials and methods) by treatment of the core with EDTA. Several rounds of dissociation were necessary to yield particles which lacked P4. A micrograph of these particles is shown in Figure 1D. The P1 particles look very similar to both the expanded PCs (Figure 1C) and empty cores (Figure 1B, white arrow).

A reconstruction was made from 18 P1 particles to 3.4 nm resolution (Figure 5E and F). Difference imaging verified that the P1 structure is remarkably similar to that of the P1, P4 expanded particle (Figure 5C and D), suggesting that the P1, P4 particle reconstruction is dominated by P1. Day and Mindich (1980) suggest that there are 120 copies of P4 per virion, based on gel electrophoresis analyses of radioactive virus, so we expected to be able to identify it. The lack of density attributable to the P4 protein raises the possibility that it may have been lost from the expanded particles. SDS–PAGE analysis showed that P4 was still present in the sample. However, it may not have been associated stoichiometrically with all of the expanded particles used in the P1, P4 reconstruction. Hence the density may have been averaged out during the reconstruction. This could also be a problem if the P4 is in a flexible conformation. Alternatively, the low resolution of the reconstructions may be limiting the differences seen.

Sequence alignment and secondary structure prediction

The P8 amino acid sequence was aligned to the VP7 amino acid sequence using the Maxhom multiple sequence alignment method (Sander and Rost, 1994) in the EMBL PredictProtein WWW server (Rost, 1996). The pairwise identity between the two sequences was 21%, with an additional 11% homology, generating the N-terminal alignment in Figure 6. When the C-terminal 263–349 residues of VP7 were used alone, the pairwise identity with P8 was only 11%, with an additional 11% homology (C-terminal alignment, Figure 6). The prediction of secondary structure was performed by a system of neural networks (Rost and Sander, 1993, 1994; Rost, 1996) using the sequence alignment between P8 and VP7. A control prediction using the 20 best hits from the PDB database of experimentally determined structures gave a similar

result for the prediction of helical secondary structure. The highest pairwise identity from this larger set was only 24%. The low homology of P8 to proteins in the three-dimensional database means that the prediction has to be interpreted with due care.

Discussion

Multi-layered segmented dsRNA viruses infect animals, plants and bacteria. Of these, the best studied examples are the Reoviridae [reovirus, rotavirus and blue tongue virus (BTV)] and the enveloped bacteriophage ϕ6. An *in vitro* system using purified components which carries out the entire RNA replication cycle has only been developed for ϕ6 (Olkkonen *et al.*, 1990). One of the reasons for the success of the ϕ6 system is that assembly of the NC is independent of non-structural viral proteins. This has allowed detailed dissection of the ssRNA binding, packaging, replication and transcription events in the assembly pathway (Gottlieb *et al.*, 1990, 1991, 1992b, 1994; Casini *et al.*, 1994; Mindich *et al.*, 1994; Frilander and Bamford, 1995; Frilander *et al.*, 1995; Qiao *et al.*, 1995; Van Dijk *et al.*, 1995).

Previous structural studies of the ϕ6 NC revealed a dodecahedral cage-like core structure (Steely and Lang, 1984; Yang and Lang, 1984). However, these studies were hampered by the fact that the particles were poorly characterized biochemically. In particular, what was considered to be the NC had actually lost several proteins because of the negative staining technique used (Ktistakis and Lang, 1987; Olkkonen and Bamford, 1987).

Here, we have used cryo-electron microscopy, which ensures the best attainable preservation of the native structure, to visualize directly the three-dimensional structure of the virus core and the NC as well as recombinant polymerase complex particles that have never packaged RNA (P1, P4 particle). This has allowed us to address the question of ϕ6 assembly from a structural point of view. We show that major structural transitions occur during assembly, and also demonstrate surprising structural similarities to other dsRNA viruses.

The T = 13 outer shell of the nucleocapsid

The NC of ϕ6 has a smooth, $T = 13$ surface structure, strikingly similar to that of equivalent substructures of other segmented dsRNA viruses. In BTV, VP7 comprises the outer layer of the core with $T = 13$ symmetry (Hewat *et al.*, 1992; Prasad *et al.*, 1992). Reovirus particles have a $T = 13$ layer consisting of two proteins, μ1 and σ3, outside the core (Metcalf *et al.*, 1991; Dryden *et al.*, 1993) and, in rotavirus, both VP6 and VP7 form smooth shells with a similar appearance to ϕ6 (Prasad *et al.*, 1988).

The structure of the VP7 trimer from BTV has been solved to high resolution by X-ray crystallography (Grimes *et al.*, 1995). The 38.5 kDa protein VP7 has two domains: a lower domain containing nine α-helices, and an upper domain consisting of a viral jelly roll motif. In the amino acid sequence, the lower α-helical domain is split into C- and N-terminal halves by the insertion of the entire upper β-sheet domain.

Raman spectroscopy experiments have shown that the ϕ6 NC coat protein P8 is mainly α-helical (Bamford *et al.*, 1993), and secondary structure prediction suggests that P8 contains seven α-helical stretches (Figure 6). The predicted α-helical regions of P8 align with four of the known N-terminal, and three of the known C-terminal α-helices of VP7 (Figure 6). Thus, one could speculate that P8 is analogous to the α-helical domain of VP7. Previous studies (Day and Mindich, 1980; Ktistakis *et al.*, 1988) and calculations from this work indicate that there could be twice as many copies of P8 as there are of the structurally equivalent proteins in the Reoviridae. However, the 16 kDa P8 protein consists of 149 amino acids, while VP7 from BTV (38.5 kDa) has 349 residues. Of the latter, 230 residues comprise the lower, α-helical domain. We suggest that two copies of P8 form the equivalent of the lower domain of VP7. Such a union of domains has been described in systems such as the comoviruses, where two viral jelly roll domains which are separate in many small RNA viruses are found as a single, two domain subunit (Chen *et al.*, 1990).

The larger diameter of the BTV $T = 13$ shell (70 nm versus the 58 nm ϕ6 NC), could reflect the projecting β-barrel domain of VP7, which would add ~8 nm to the diameter of the BTV shell (Grimes *et al.*, 1995). In reovirus, μ1 (76 kDa) forms a $T = 13$ shell, while σ3 comprises finger-like protrusions on the outside of the μ1 layer (Dryden *et al.*, 1993). The outer surface of the inner capsid of rotavirus appears most similar to the ϕ6 NC. This surface contains 780 copies of the rotavirus VP6 (45 kDa) (Yeager *et al.*, 1994). In addition to these similarities in the $T = 13$ shell, all of these viruses also share a number of similarities in the core (see below).

Polymerase complexes of dsRNA viruses

Mindich and Bamford (1988) used measurements of the amounts of proteins in the ϕ6 virion and NC (Van Etten *et al.*, 1976; Day and Mindich, 1980) to formulate a model in which 120 copies of P1 form the main structural framework of the virus, with a dimer of P1 comprising the basic subunit. The structure shows that P1 forms not only the 30 bars of the dodecahedron (Figure 5A and E) but also the mass on the 12 faces. At the present resolution, individual subunits cannot be delineated, but volume measurements indicate that a copy number of 120 is very likely.

Although 120 is an unusual number of subunits of a structural protein for an icosahedral particle, it is not unique to this system. The LA virus of yeast (Cheng *et al.*, 1994) and the cores of several of the Reoviridae contain 120 copies of at least one major structural protein. This includes the BTV VP3 (103 kDa; Burroughs *et al.*, 1995) and the reovirus λ1 (137 kDa; Schiff and Fields, 1990). In both of these systems, the core particle is transcriptionally active and hence functionally equivalent to the ϕ6 core. Thus, a common structural theme is seen even though the only major sequence similarity that has been noted between ϕ6 and other segmented dsRNA viruses is in the polymerase active sites (Bruenn, 1991). Both BTV VP3 particles (Huismans *et al.*, 1987) and rotavirus cores (Labbé *et al.*, 1991; Prasad *et al.*, 1996) have a similar outline to the P1 particle described here. The polymerase of rotavirus recently has been localized to the 5-fold axes of symmetry, suggesting that this is a crucial site for the synthesis of RNA (Prasad *et al.*, 1996). Like ϕ6, the reovirus core also has protruding turrets situated on the

5-fold axes of symmetry (Metcalf *et al.*, 1991; Dryden *et al.*, 1993). Evidence from micrographs of transcribing reovirus cores (Bartlett *et al.*, 1974) indicates that these turrets are the site of exit of the newly synthesized ssRNA. The ϕ6 core has ~2 nm wide channels through the centre of its turrets which could serve the same function (Figure 3B). Thus, by analogy, the minor ϕ6 core proteins such as the polymerase may also be located here, but further work is required to confirm this.

The striking higher order structural features shared between ϕ6 and the other dsRNA viruses suggest either that similarities in replication strategies have resulted in a similar structural solution or that the entire set of dsRNA viruses share a common ancestor.

The ϕ6 assembly pathway

Proteins P1, P2, P4 and P7 comprise the ϕ6 PC. The minimum requirement for particle assembly appears to be the presence of both P1 and P4, as expression of P1 alone in *E.coli* leads to unstable particles and non-specific aggregation (Gottlieb *et al.*, 1988b).

The PC recognizes and packages the three segments of plus sense ssRNA. All three strands need to be packaged before minus strand synthesis can commence (Gottlieb *et al.*, 1992b). After minus strand synthesis, the dsRNA-containing particle (polymerase complex) is active in transcription and is therefore equivalent to the core that can be isolated from the NC. Furthermore, the PC only seems to be able to act as a template for the assembly of P8 after packaging and minus strand synthesis (Olkkonen *et al.*, 1991). This strictly sequential course of events points to the involvement of conformational changes in the transition from RNA-naive PC to NC.

Structural rearrangements of the ϕ6 PC are evident when micrographs of the PC are compared with those of cores isolated from the virion (Figure 1C and D) The reconstructions of these two types of particles (Figures 3 and 5) make the nature of the change more obvious. The core particle found inside the virion represents an expanded form of the polymerase complex. The PC produced in *E.coli* is an unexpanded, precursor form. The extent of this flexibility is illustrated schematically in Figure 7. The movement seems to be hinged at the 2-fold axes (12 and 6 o'clock positions of Figure 7) where least change is seen, but allowing up to a 19 nm movement at the centre of the 5-fold axes (3 o'clock position of Figure 7). Thus an important conclusion from the P1, core and PC reconstructions is that P1 has at least three possible conformations. The two most extreme (PC and core) are known to be functional in the life cycle.

This expansion is analogous to the maturation process found in the dsDNA viruses (Hendrix and Garcea, 1994). Normally, such expansion would take place upon nucleic acid packaging (or upon production of the minus strands). However, expansion in ϕ6 could also be triggered spontaneously by gentle heat treatment. Such metastability would drive the assembly toward the final product. In the dsDNA phages, expansion can often be triggered by high salt, chaotropic agents or similar treatments, and is completely irreversible. In ϕ6, however, complete expansion can apparently only be attained by a bona fide packaging event, since the expanded PC is in an intermediate state between the PC and the dsRNA-containing

Fig. 7. Flexibility of the polymerase complex. The diagram shows the relative positions of the PC shell (navy blue), the P1 shell or expanded P1, P4 shell (brown) and the core (yellow/green). The arrows indicate the possible movement of each shell. The PC can expand to position 1, and may expand to position 2 when it contains dsRNA. The core seems to contract to position 1 when it loses its dsRNA.

core (Figure 7). Furthermore, the core is still flexible, as loss of RNA causes the core to collapse (Figures 3, 5 and 7), as evidenced by the structure of the isolated P1 particle (Figure 5C and F) and the empty core (Figure 1B, white arrow). This collapsed state corresponds almost exactly to the *in vitro* expanded form of the PC (Figure 5B and E).

Major structural arrangements upon genome packaging are a feature of many viral systems (Dokland and Murialdo, 1993; Prasad *et al.*, 1993; Ilag *et al.*, 1995). During the partial expansion of the P1, P4 particle, the dodecahedral cage takes on an inflated appearance, and the cups turn into shallow dishes as the segments that make up the cup move radially outwards into the surface plane (Figures 5 and 7). The completely expanded core particle has an almost completely spherical shell, and the turrets have taken the place of the cups (Figures 3 and 7).

The expansion of the PC is a requirement for P8 assembly. Olkkonen *et al.* (1991) showed that purified P8 could be reassembled onto cores isolated from the virion, but not onto PCs. The core turrets, which extend out to the surface of the NC only after complete expansion of

the PC, are at the right position for nucleating the assembly of P8 in a calcium ion-dependent reaction. P8 self-assembly, i.e. in the absence of expanded cores, leads to the formation of multi-lamellar aberrant structures (Ktistakis *et al.*, 1988). Clearly, the core acts as both a nucleation site and a regulator of P8 assembly. This may be analogous to the portal proteins or scaffolding proteins of dsDNA phages, without which aberrant assemblies are often produced (Earnshaw and King, 1978; Guo *et al.*, 1991). The binding of P8 itself may in turn induce additional conformational changes in the core proteins, such as the contacts that appear near the 2-fold axis between the P8 shell and the core inside the NC (Figure 4C). It will certainly affect the accessibility of the core proteins to monoclonal antibodies as described previously (Ojala *et al.*, 1993, 1994).

The assembly of ϕ6 is a complex, multi-step process. The present structures represent a beginning on the road to understanding the exact sequence of events leading to the complete multi-functional ϕ6 virion. In addition, structural studies of the enveloped forms of ϕ6 should provide further insight into the events which take place during entry and maturation.

Materials and methods

Isolation of NC and core particles

Bacteriophage ϕ6 was grown on *P.syringae* pv. *phaesolicola* HB10Y (Vidaver *et al.*, 1973) as described previously (Olkkonen *et al.*, 1991; Ojala *et al.*, 1993).

Purified ϕ6 virions were treated with 4 mM butylated hydroxytoluene (BHT) which removes the spike protein, P3, and stored at –70°C until required. The envelope of the BHT-treated particles was solubilized by treatment with Triton X-114, yielding the NC as described previously (Ojala *et al.*, 1993).

Cores were isolated from NCs by the addition of EGTA which releases the NC surface protein, P8 (Olkkonen *et al.*, 1991). To stabilize the cores, 1 mM GTP was added to the uncoating reaction buffer and the uncoating gradient (Ojala *et al.*, 1994). Storage of the preparation on ice led to gradual loss of RNA from the particles. Accordingly, specimens were vitrified immediately after preparation.

Purification of P1 particles

The isolation of P1 particles from disrupted NCs was adapted from that published earlier (Olkkonen and Bamford, 1987). ϕ6 virions were purified as described (Ojala *et al.*, 1993) except that 8% polyethyleneglycol (PEG), 0.5 M NaCl was used in precipitation of the bacteriophage. This reduction in the PEG concentration gave rise to less stable virions and resulted in a higher yield of P1 particles. NCs were isolated from the virions as described previously (Ojala *et al.*, 1993). The resuspended NC pellet was applied to a second 5–20% sucrose gradient in 20 mM Tris–HCl pH 8, 1 mM $MgCl_2$ (30 000 r.p.m., 15°C, 50 min, Beckman SW40 rotor). The NC band was harvested and stored overnight on ice. The NCs were collected by centrifugation in a Beckman airfuge (29 p.s.i., 8 min, 20°C, Beckman A-100/18 rotor), and resuspended in 45% of the initial volume, in 20 mM Tris–HCl pH 7.5. In order to remove the remaining proteins from the P1 cage, EDTA (pH 8.0) was added to a final concentration of 11 mM and the particles were incubated for 30 min at 23°C. The resulting P1 particles were then loaded onto a 5–20% sucrose gradient containing 20 mM Tris–HCl pH 7.5, 10 mM EDTA and 0.75 M NaCl and centrifuged (30 000 r.p.m., 15°C, 50 min, SW40 rotor). The light-scattering band was harvested and the particles collected in a Beckman airfuge (29 p.s.i., 8 min, 20°C, Beckman A-100/18 rotor). The P1 samples were analysed by immunoblotting to ensure that only P1 was present.

Isolation of polymerase complexes in E.coli

PCs were produced using the expression plasmid pLM450 (Gottlieb *et al.*, 1990) propagated in *E.coli* JM109 in the presence of 10 μg/ml tetracycline. PC-related particles containing only proteins P1 and P4 were produced using the expression plasmid pLM358 and 150 μg/ml ampicillin (Gottlieb *et al.*, 1990). Purification of PCs was as previously described (Frilander and Bamford, 1995).

Electron microscopy

Samples were concentrated in a Beckman airfuge and resuspended in 10 mM NaCl, 20 mM Tris–HCl pH 7.5 immediately before vitrification, and prepared as described previously (Cyrklaff *et al.*, 1990; Dokland and Murialdo, 1993; Butcher *et al.*, 1995). Most of the images were obtained using a Philips 400 electron microscope at 80 kV with a magnification of 34 400×. The cores and P1 particles were observed in a Philips CM200 electron microscope equipped with a field emission gun operating at 200 kV, at a magnification of 38 000×. GATAN cryo-specimen holders operating at a temperature of about –175°C were used in both electron microscopes. The images used were taken with underfocus values between 1.6 and 3.2 μm as confirmed by optical diffraction.

Image processing

The micrographs were digitized on a Perkin-Elmer 1010GM flat-bed scanner with a pixel size ranging of 22 μm corresponding to ~6.4 nm on the film (P1 and PC particles), 25 μm corresponding to ~0.75 nm (NC) and 19 μm corresponding to ~0.5 nm (cores). Initial image processing and icosahedral reconstruction were performed as described previously (Butcher *et al.*, 1995). Once a reasonable reconstruction was generated using orientations determined by common-lines procedures (Crowther, 1971; Fuller *et al.*, 1996), this reconstruction was used in a correlation search to test the reliability of orientations and to orient additional particles (Baker and Cheng, 1996). The same model could be used to orient other structurally related particles. The orientations and centres of a whole set of particles were then refined using cross-common lines refinement (Fuller *et al.*, 1996) after excluding particles that showed high phase residuals. The final reconstructions were made to a resolution justified by the phase residual. The particle orientations for each reconstruction were distributed throughout the asymmetric unit triangle, and in all cases the coverage of data in Fourier space was more than sufficient for the resolution used, as all inverse Eigenvalues were <1.0, and at least 95% were <0.1 (Crowther, 1971). At least two data sets from different micrographs and different preparations were processed for each reconstruction. The features described here were consistent between the data sets. Programs were run on a DEC 7000 AXP and a VAX 9000. Advanced Visualisation System (AVS) version 5 software was used to visualize the final reconstructions on Silicon Graphics workstations. To calculate difference images, the two maps to be compared were calculated to the same resolution, scaled for differences in pixel size and subtracted using the AVS module, norm_3d (Vénien-Bryan and Fuller, 1994). The icosahedral programs used are described at http://www.EMBL-Heidelberg.DE/ExternalInfo/fuller/ and are available upon request.

Acknowledgements

We are pleased to acknowledge the contributions of Dr J.Kenney (London) and Dr J.Kankare (Helsinki) who made the early reconstructions of the P1 cage and polymerase complex. We also thank M.Cyrklaff (Strasbourg) and B.Gowen (EMBL) for help with the microscopy of ϕ6 particles, and Dr L.Mindich (New York) for the L segment clones and *E.coli* strains used in the procapsid assembly experiments. We are also indebted to Dr David Stuart (Oxford) and Dr L.Mindich (New York) for many useful discussions. Dr P.Metcalf (Palmiston North), R.Heinkel (EMBL), Dr T.Baker (Purdue) and Dr R.H.Cheng (Stockholm) are thanked for graciously sharing their programs. S.J.B. and T.D. were supported by a European Union Science network grant (ERBSC1* CT000735). D.H.B. was supported by the Finnish Academy of Sciences. A portion of this work was supported by a European Union Access to Large Scale Facilities grant (ERBCHGECT940062).

References

Adrian,M., Dubochet,J., Lepault,J. and McDowall,A.W. (1984) Cryo-electron microscopy of viruses. *Nature*, **308**, 32–36.

Baker,T.S. and Cheng,R.H. (1996) A model-based approach for determining orientations of biological macromolecules imaged by cryo-electron microscopy. *J. Struct. Biol.*, **116**, 120–130.

Bamford,D.H. and Wickner,R.B. (1994) Assembly of double-stranded RNA viruses: bacteriophage ϕ6 and yeast virus L-A. *Semin. Virol.*, **5**, 61–69.

Bamford,D.H., Palva,E.T. and Lounatmaa,K. (1976) Ultrastructure and life cycle of the lipid-containing bacteriophage ϕ6. *J. Gen. Virol.*, **32**, 249–259.

Bamford,D.H., Romantschuk,M. and Somerharju,P.J. (1987) Membrane fusion in prokaryotes: bacteriophage ϕ6 membrane fuses with the *Pseudomonas syringae* outer membrane. *EMBO J.*, **6**, 1467–1473.

Bamford,J.K.H., Bamford,D.H., Li,T. and Thomas,G.J. (1993) Structural studies of the enveloped dsRNA bacteriophage ϕ6 of *Pseudomonas syringae* by Raman spectroscopy. II. Nucleocapsid structure and thermostability of the virion, nucleocapsid and polymerase complex. *J. Mol. Biol.*, **230**, 473–482.

Bartlett,N.M., Gillies,S.C., Bullivant,S. and Bellamy,A.R. (1974) Electron microscopy study of reovirus reaction cores. *J. Virol.*, **14**, 315–326.

Bruenn,J.A. (1991) Relationships among the positive strand and double-strand RNA viruses as viewed through their RNA-dependent RNA polymerases. *Nucleic Acids Res.*, **19**, 217–226.

Burroughs,J.N., Grimes,J., Mertens,P.P.C. and Stuart,D.I. (1995) Crystallization and preliminary X-ray analysis of the core particle of bluetongue virus. *Virology*, **210**, 217–220.

Butcher,S.J., Bamford,D.H. and Fuller,S.D. (1995) DNA packaging orders the membrane of bacteriophage PRD1. *EMBO J.*, **14**, 6078–6086.

Casini,G., Qiao,X. and Mindich,L. (1994) Reconstitution of active replicase in procapsids of the segmented dsRNA bacteriophage ϕ6. *Virology*, **204**, 251–253.

Caspar,D.L.D. and Klug,A. (1962) Physical principles in the construction of regular viruses. *Cold Spring Harbor Symp. Quant. Biol.*, **27**, 1–24.

Chen,Z., Stauffacher,C.V. and Johnson,J.E. (1990) Capsid structure and RNA packaging in comoviruses. *Semin. Virol.*, **1**, 453–466.

Cheng,R.H. *et al*. (1994) Fungal virus capsids, cytoplasmic compartments for the replication of double-stranded RNA, formed as icosahedral shells of asymmetric Gag dimers. *J. Mol. Biol.*, **244**, 255–258.

Crowther,R.A. (1971) Procedures for three-dimensional reconstruction of spherical viruses by Fourier synthesis from electron micrographs. *Philos. Trans. R. Soc. Lond., B.*, **261**, 221–230.

Cyrklaff,M., Adrian,M. and Dubochet,J. (1990) Evaporation during preparation of unsupported thin vitrified aqueous layers for cryo-electron microscopy. *J. Electron Microsc. Techn.*, **16**, 351–355.

Day,L.A. and Mindich,L. (1980) The molecular weight of bacteriophage ϕ6 and its nucleocapsid. *Virology*, **103**, 376–385.

Dokland,T. and Murialdo,H. (1993) Structural transitions during maturation of bacteriophage lambda capsids. *J. Mol. Biol.*, **233**, 682–694.

Dryden,K.A., Wang,G., Yeager,M., Nibert,M.L., Coombs,K.M., Furlong,D.B., Fields,B.N. and Baker,T.S. (1993) Early steps in reovirus infection are associated with dramatic changes in supramolecular structure and protein conformation: analysis of virions and subviral particles by cryoelectron microscopy and image reconstruction. *J. Cell Biol.*, **122**, 1023–1041.

Dubochet,J., Adrian,M., Chang,J.-J., Homo,J.-C., Lepault,J., McDowall, A.W. and Schultz,P. (1988) Cryo-electron microscopy of vitrified specimens. *Q. Rev. Biophys.*, **21**, 129–228.

Earnshaw,W. and King,J. (1978) Structure of phage P22 coat protein aggregates formed in the absence of the scaffolding protein. *J. Mol. Biol.*, **126**, 721–747.

Frilander,M. and Bamford,D.H. (1995) *In vitro* packaging of the single-stranded RNA genomic precursors of the segmented double-stranded RNA bacteriophage ϕ6: the three segments modulate each other's packaging efficiency. *J. Mol. Biol.*, **246**, 418–428.

Frilander,M., Poranen,M. and Bamford,D.H. (1995) The large genome segment of dsRNA bacteriophage ϕ6 is the key regulator in the *in vitro* minus and plus strand synthesis. *RNA*, **1**, 510–518.

Fuller,S.D., Butcher,S.J., Cheng,R.H. and Baker,T.S. (1996) Three-dimensional reconstruction of icosahedral particles—the uncommon line. *J. Struct. Biol.*, **116**, 48–55.

Gottlieb,P., Metzger,S., Romantschuk,M., Carton,J., Strassman,J., Bamford,D.H., Kalkkinen,N. and Mindich,L. (1988a) Nucleotide sequence of the middle dsRNA segment of bacteriophage ϕ6: placement of the genes of membrane-associated proteins. *Virology*, **163**, 183–190.

Gottlieb,P., Strassman,J., Bamford,D. and Mindich,L. (1988b) Production of a polyhedral particle in *Escherichia coli* from a cDNA copy of the large genome segment of ϕ6. *J. Virol.*, **62**, 181–187.

Gottlieb,P., Strassman,J., Quao,X., Frucht,A. and Mindich,L. (1990) *In vitro* replication, packaging, and transcription of the segmented, double-stranded RNA genome of bacteriophage ϕ6: studies with procapsids assembled from plasmid-encoded proteins. *J. Bacteriol.*, **172**, 5774–5782.

Gottlieb,P., Strassman,J., Frucht,A., Quao,X. and Mindich,L. (1991) *In vitro* packaging of the bacteriophage ϕ6 ssRNA genomic precursors. *Virology*, **181**, 589–594.

Gottlieb,P., Strassman,J. and Mindich,L. (1992a) Protein P4 of the bacteriophage ϕ6 procapsid has a nucleoside triphosphate-binding site with associated nucleoside triphosphate phosphohydrolase activity. *J. Virol.*, **66**, 6220–6226.

Gottlieb,P., Strassman,J., Qiao,X., Frilander,M., Frucht,A. and Mindich,L. (1992b) *In vitro* packaging and replication of individual genomic segments of bacteriophage ϕ6 RNA. *J. Virol.*, **66**, 2611–2616.

Gottlieb,P., Qiao,X., Strassman,J., Frilander,M. and Mindich,L. (1994) Identification of the packaging regions within the genomic RNA segments of bacteriophage ϕ6. *Virology*, **200**, 42–47.

Grimes,J., Basak,A.K., Roy,P. and Stuart,D. (1995) The crystal structure of bluetongue virus VP7. *Nature*, **373**, 167–170.

Guo,P., Erickson,S., Xu,W., Olson,N., Baker,T.S. and Anderson,D. (1991) Regulation of the phage ϕ29 prohead shape and size by the portal vertex. *Virology*, **183**, 366–373.

Hendrix,R.W. and Garcea,R.L. (1994) Capsid assembly of dsDNA viruses. *Semin. Virol.*, **5**, 15–26.

Hewat,E.A., Booth,T.F. and Roy,P. (1992) Structure of bluetongue virus particles by cryoelectron microscopy. *J. Struct. Biol.*, **109**, 61–69.

Huismans,H., Van Dijk,A.A. and Els,H.J. (1987) Uncoating of parental bluetongue virus to core and subcore particles in infected L cells. *Virology*, **157**, 180–188.

Ilag,L.L. *et al*. (1995) DNA packaging intermediates of bacteriophage phiX174. *Structure*, **3**, 353–363.

Juuti,J.T. and Bamford,D.H. (1995) RNA binding, packaging and polymerase activities of the different incomplete polymerase complex particles of dsRNA bacteriophage ϕ6. *J. Mol. Biol.*, **249**, 545–554.

Kakitani,H., Iba,H. and Okada,Y. (1980) Penetration and partial uncoating of bacteriophage ϕ6 particle. *Virology*, **101**, 475–483.

Koonin,E.V., Gorbalenya,A.E. and Chumakov,K.M. (1989) Tentative identification of RNA-dependent RNA polymerases of dsRNA viruses and their relationship to positive strand RNA viral polymerases. *FEBS Lett.*, **252**, 42–46.

Ktistakis,N.T. and Lang,D. (1987) The dodecahedral framework of the bacteriophage ϕ6 nucleocapsid is composed of P1. *J. Virol.*, **61**, 2621–2623.

Ktistakis,N.T., Kao,C. and Lang,D. (1988) *In vitro* assembly of the outer shell of bacteriophage ϕ6 nucleocapsid. *Virology*, **166**, 91–102.

Labbé,M., Charpilienne,A., Crawford,S.E., Estes,M.K. and Cohen,J. (1991) Expression of rotavirus VP2 produces empty corelike particles. *J. Virol.*, **65**, 2946–2952.

McGraw,T., Mindich,L. and Frangione,B. (1986) Nucleotide sequence of the small double-stranded RNA segment of bacteriophage ϕ6: novel mechanism of natural translational control. *J. Virol.*, **58**, 142–151.

Metcalf,P., Cyrklaff,M. and Adrian,M. (1991) The three-dimensional structure of reovirus obtained by cryo-electron microscopy. *EMBO J.*, **10**, 3129–3136.

Mindich,L. and Bamford,D.H. (1988) Lipid containing bacteriophages. In Calendar,R. (ed.), *The Bacteriophages*. Plenum, New York, Vol. 2, pp. 475–520.

Mindich,L. and Davidoff-Abelson,R. (1980) The characterization of a 120S particle formed during ϕ6 infection. *Virology*, **103**, 386–391.

Mindich,L., Nemhauser,I., Gottlieb,P., Romantschuk,M., Carton,J., Frucht,S., Strassman,J., Bamford,D.H. and Kalkkinen,N. (1988) Nucleotide sequence of the large double-stranded RNA segment of bacteriophage ϕ6: genes specifying the viral replicase and transcriptase. *J. Virol.*, **62**, 1180–1185.

Mindich,L., Qiao,X., Onodera,S., Gottlieb,P. and Frilander,M. (1994) RNA structural requirements for stability and minus-strand synthesis in the dsRNA bacteriophage ϕ6. *Virology*, **202**, 258–263.

Ojala,P.M., Romantschuk,M. and Bamford,D.H. (1990) Purified ϕ6 nucleocapsids are capable of productive infection of host cells with partially disrupted outer membranes. *Virology*, **178**, 364–372.

Ojala,P.M., Juuti,J.T. and Bamford,D.H. (1993) Protein P4 of double-stranded RNA bacteriophage ϕ6 is accessible on the nucleocapsid surface: epitope mapping and orientation of the protein. *J. Virol.*, **67**, 2879–2886.

Ojala,P.M., Paatero,A.O. and Bamford,D.H. (1994) NTP binding induces conformational changes in the double-stranded RNA bacteriophage ϕ6 subviral particles. *Virology*, **205**, 170–178.

Olkkonen,V.M. and Bamford,D.H. (1987) The nucleocapsid of the lipid containing double stranded bacteriophage ϕ6 contains a protein skeleton consisting of a single polypeptide species. *J. Virol*., **61**, 2362–2367.

Olkkonen,V.M., Gottlieb,P., Strassman,J., Qiao,X.Y., Bamford,D.H. and Mindich,L. (1990) *In vitro* assembly of infectious nucleocapsids of bacteriophage ϕ6: formation of a recombinant double-stranded RNA virus. *Proc. Natl Acad. Sci. USA*, **87**, 9173–9177.

Olkkonen,V.M., Ojala,P.M. and Bamford,D.H. (1991) Generation of infectious nucleocapsids by *in vitro* assembly of the shell protein on to the polymerase complex of the dsRNA bacteriophage ϕ6. *J. Mol. Biol*., **218**, 569–581.

Prasad,B.V.V., Wang,G.J., Clerx,J.P.M. and Chiu,W. (1988) Three-dimensional structure of rotavirus. *J. Mol. Biol*., **199**, 269–275.

Prasad,B.V., Yamaguchi,S. and Roy,S. (1992) Three-dimensional structure of single-shelled bluetongue virus. *J. Virol*., **66**, 2135–2142.

Prasad,B.V.V., Prevelige,P.E., Marietta,E., Chen,R.O., Thomas,D., King,J. and Chiu,W. (1993) Three-dimensional transformation of capsids associated with genome packaging in a bacterial virus. *J. Mol. Biol*., **231**, 65–74.

Prasad,B.V.V., Rothnagel,R., Zeng,C.Q.-V., Jakana,J., Lawton,J.A., Chiu,W. and Estes,M.K. (1996) Visualization of ordered genomic RNA and localization of transcriptional complexes in rotavirus. *Nature*, **382**, 471–473.

Qiao,X., Qiao,J. and Mindich,L. (1995) Interference of bacteriophage ϕ6 genomic RNA packaging by hairpin structures. *J. Virol*., **69**, 5502–5505.

Revel,H.R., Ewen,M.E., Brusslan,J. and Pagratis,N. (1986) Generation of cDNA clones of the bacteriophage ϕ6 segmented dsRNA genome: characterization and expression of L segment clones. *Virology*, **155**, 402–417.

Romantschuk,M., Olkkonen,V.M. and Bamford,D.H. (1988) The nucleocapsid of bacteriophage ϕ6 penetrates the host cytoplasmic membrane. *EMBO J*., **7**, 1821–1829.

Rost,B. (1996) PHD: predicting one-dimensional protein structure by profile based neural networks. *Methods Enzymol*., **266**, 525–539.

Rost,B. and Sander,C. (1993) Secondary structure prediction of all-helical proteins in two states. *Protein Engng*, **6**, 831–836.

Rost,B. and Sander,C. (1994) Combining evolutionary information and neural networks to predict protein secondary structure. *Proteins*, **19**, 55–72.

Sander,C. and Rost,B. (1994) The HSSP data base of protein structure–sequence alignments. *Nucleic Acids Res*., **22**, 3597–3599.

Schiff,L.A. and Fields,B.N. (1990) Reoviruses and their replication. In Fields,B.N., Knipe,D.M., Chanock,R.M., Hirsch,M.S., Melnick,J.L., Monath,T.P. and Roizman,B. (eds), *Virology.* Raven Press, New York, Vol. 2, pp. 1275–1306.

Semancik,J.S., Vidaver,A.K. and Van Etten,J.L. (1973) Characterization of a segmented double-helical RNA from bacteriophage ϕ6. *J. Mol. Biol*., **78**, 617–625.

Steely,H.T. and Lang,D. (1984) Electron microscopy of the bacteriophage ϕ6 nucleocapsid: two dimensional image analysis. *J. Virol.*, **51**, 479–483.

Stewart,P.L., Burnett,R.M., Cyrklaff,M. and Fuller,S.D. (1991) Image reconstruction reveals the complex molecular organization of adenovirus. *Cell*, **67**, 145–154.

Van Dijk,A.A., Frilander,M. and Bamford,D.H. (1995) Differentiation between minus- and plus-strand synthesis: polymerase activity of dsRNA bacteriophage ϕ6 in an *in vitro* packaging and replication system. *Virology*, **211**, 320–323.

Van Etten,J.L., Vidaver,A.K., Koski,R.K. and Burnett,J.P. (1974) Base composition and hybridization studies of the three double-stranded RNA segments of bacteriophage ϕ6. *J. Virol*., **13**, 1254–1262.

Van Etten,J.L., Lane,L., Gonzales,C., Partridge,J. and Vidaver,A. (1976) Comparative properties of bacteriophage ϕ6 and ϕ6 nucleocapsid. *J. Virol*., **18**, 652–658.

Vénien-Bryan,C. and Fuller,S.D. (1994) The organization of the spike complex of Semliki Forest virus. *J. Mol. Biol*., **236**, 572–583.

Vidaver,A.K., Koski,R.K. and Van Etten,J.L. (1973) Bacteriophage ϕ6: a lipid-containing virus of *Pseudomonas phaseolicola*. *J. Virol*., **11**, 799–805.

Yang,Y. and Lang,D. (1984) Electron microscopy of bacteriophage ϕ6 nucleocapsids: three-dimensional image analysis. *J. Virol*., **51**, 484–488.

Yeager,M., Berrimann,J.A., Baker,T.S. and Bellamy,A.R. (1994) Three-dimensional structure of the rotavirus hemagglutinin VP4 by cryo-electron microscopy and difference map analysis. *EMBO J*., **13**, 1011–1018.

Received on February 19, 1997; revised on April 10, 1997